Nat. Hazards Earth Syst. Sci. Discuss., 1, 5603–5641, 2013
www.nat-hazards-earth-syst-sci-discuss.net/1/5603/2013/
doi:10.5194/nhessd-1-5603-2013

Natural Hazards and Earth System Sciences
Open Access
Discussions

Sensitivity of the WRF model to the lower boundary in an extreme precipitation event – Madeira Island case study

J. C. Teixeira [1], A. C. Carvalho[2], T. Luna[3], and A. Rocha[1]

[1]Department of Physics, CESAM, University of Aveiro, Campus Universitario de Santiago 3810-193 Aveiro, Portugal
[2]CENSE, Departament of Science Environmental Engineering, Faculdade de Ciências e Tecnologia, Universidade Nova de Lisboa, 2829-516 Caparica, Portugal
[3]IDAD The Institute for Environment and Development, Campus Universitario de Santiago 3810-193 Aveiro, Portugal

Received: 2 August 2013 – Accepted: 10 September 2013 – Published: 16 October 2013

Correspondence to: J. C. Teixeira (jcmt@ua.pt)

Published by Copernicus Publications on behalf of the European Geosciences Union.

Abstract

Through the years, the advances in satellite technology made feasible the acquisition of information about the Earth surface, such as elevation and land use with great detail and resolution. This information can be included in numerical atmospheric models, updating them and providing a more detailed lower boundary, which in turn can improve the results of events forced by it. Given this, this work aims to study the sensitivity of the Weather Research and Forecast model to three different topography datasets as well as two different land use datasets in an extreme precipitation event. A test case study in which topography driven precipitation was dominant over Madeira Island was considered which triggered several flash floods and mudslides in the southern parts of the island. Model results show higher model skill in precipitation over Madeira leeward and in the windward wind flow, in spite of the non significant enhancement on the overall results with higher resolution datasets of topography and land use.

1 Introduction

Topography plays an important role in atmospheric dynamics as it can force flow dynamics, precipitation patterns and change atmospheric water vapour concentration. Given this, the influence of topography on water vapour transport and the different forcing mechanisms, acting on different time and length scales, that can produce orographic precipitation has been the focus of several studies for the past decades.

Due to the complexity of topographic forced mechanisms, studies concerning idealised situation such as the uniformly stratified moist flow over a Gaussian-shaped circular mountain, have been performed by several authors, namely Jiang (2003); Colle (2004); Kunz and Kottmeier (2006a). These works perform sensitivity studies in order to determine the relationship between the mountain's dimension and the precipitation intensity and distribution.

Under these assumptions and using a mesoscale model, Jiang (2003) and Colle (2004) studied the interaction between flow stagnation and orographic precipitation. In their work the authors showed that there is a significant relationship between the flow blocking and splitting effect and precipitation distribution and intensity. For low mountains the upslope ascent is dominant and the precipitation intensity is proportional to the mountain height and wind speed. On the other hand, for high mountains the flow tends to pass around the barrier, reducing the lift effect. With regard to model parameters, Kunz and Kottmeier (2006a) showed that the results are less sensitive to model parameterizations than to ambient conditions.

In addition to idealised studies, abundant real case studies have been performed concerning the effect of mountain barriers in climate, interaction with synoptic scale processes or even studies of single cases of extreme orographic precipitation (Kunz and Kottmeier, 2006b; Maussion et al., 2011). Furthermore, atmospheric numerical models have been found to be useful in order to assess precipitation in areas where observations are scarce and estimates are difficult (Maussion et al., 2011). As Vrochidou and Tsanis (2012) showed in a multi-year study, the precipitation patterns found in the Crete Island (Greece) have a strong correlation with the island topography. This connection was found to be an important clue for spatial drought patterns. Concerning the synoptic scale interaction, Ghafarian et al. (2012) studied the effects of the Anatolian and Caucasus mountains on the precipitation distribution over the Black Sea. For their research the authors performed the numerical simulation of a precipitating synoptic system passing through the study area. Using two different configurations, one with all the topographic features and the other in which the mountains were removed. These authors concluded that although there was a significant change in the fields of vertical motion, relative vorticity, humidity, low level geopotential height, cloud water content and precipitation distribution, the mountains were not responsible for the cyclogenesis.

Considering that topography plays an important role in flow and precipitation patterns, Shi et al. (2008) conducted a topography sensitivity study, for the Tibetan

Plateau. In one simulation the authors used a topography resolution consistent with the numerical model spatial resolution 30 km and in the other, a 120 km resolution topography that was then interpolated in order to be consistent with the model grid. Model results showed that the simulation with higher resolution topography agreed with the observed precipitation. On the other hand, the simulation that used the coarser resolution, considerably underestimates the observed precipitation. Besides the effects of topography changes in flow and precipitation patterns Chen et al. (2001) showed how lower boundary conditions, for example soil moisture and land use, may affect precipitation and convection in a flash flood case study. Couto et al. (2012) identified and studied four cases of intense precipitation over Madeira Island during the winter of 2009/2010 using both observed and simulated data. In their work the authors concluded that Madeira's orography is the dominant factor both in the formation and intensification of precipitation, being the altitude the main factor contributing to the precipitation distribution.

Even though the numerous works concerning topographic forcing in precipitation, little it is known about the influence of different high resolution lower boundary datasets in modelled results. Also, using observed data Fragoso et al. (2012) has characterised the rainfall and the synoptic setting of the 20 February 2010 flash-floods in Madeira focusing on the dynamical conditions that promoted the extreme precipitation event.

In the study presented here, a mesoscale numerical weather prediction model was used to assess the sensitivity of the model's lower boundary conditions to an extreme precipitation event. The chosen event occurred on the morning of the 20 February 2010 over the Madeira Island. This event was associated to a frontal system, embedded in a depression centred over the Azores archipelago, and moving to the northeast. The occurred precipitation intensity triggered flash floods and mudslides, which had important social and economic consequences. Over 40 people died in the event and several houses and structures were damaged or destroyed.

Previous work had already studied the ability of numerical models to forecast this extreme precipitation event (Grumm, 2010; Luna et al., 2011), namely Grumm (2010) who analysed the ability of the National Center for Environmental Prediction of the United States of America ensemble Global Forecasting System (GFS) to forecast this event and concluded that the pattern associated to the heavy precipitation event over Madeira was well predicted. Also Luna et al. (2011) found that orography was the main factor explaining the precipitation event's amplitude and phase over the island. Furthermore, it was shown in this work that horizontal resolution is an important factor when simulating local precipitation.

2 Methods and data

The numerical model used in this work is the Weather Research and Forecasting – Advance Research model (WRF-ARW) version 3.3 (Skamarock et al., 2008). Initial and lateral boundary conditions from GFS analyses (NCEP, 2003) were provided to the model at a six hour interval. The GFS model has an approximated horizontal resolution of $0.5^\circ \times 0.5^\circ$ that extends vertically from the 1000 to 0.27 hPa in 64 unequally spaced model levels.

The Madeira Island is located in the Atlantic Ocean South-west of mainland Portugal – Fig. 1. It has a mountain ridge extending along the central part of the island reaching a maximum altitude of 1862 m – Pico Ruivo.

Three two-way nested domains were applied to the study area – Fig. 2. The parent domain (d01) with horizontal resolution of 25 km, and two nested domains (d02 and d03) with an horizontal resolution of 5 and 1 km, respectively. The simulated period was 24 h, starting on 20 February 2010.

The set of parameterizations which were used in the present study was the same that Luna et al. (2011) used for the same event. Therefore, the following schemes were used: WRF Single-Moment 6-class scheme microphysics (Hong and Lim, 2006), Goddard shortwave radiation (Chou and Suarez, 2001), Rapid Radiative Transfer Model (RRTM) longwave radiation model (Mlawer et al., 1997), the Eta similarity surface layer scheme (Janjić, 2002), Mellor–Yamada–Janjic planetary boundary layer scheme (Janjić, 1990) and the Noah Land Surface Model (Chen and Dudhia, 2001). Cumulus have been resolved explicitly as by Luna et al. (2011) who showed that cumulus parameterization is not relevant to simulated precipitation in this particular event.

In order to conduct sensitivity tests to the topography and land use, several experiments were performed. In these experiments two topography datasets – The The Shuttle Radar and Topography Mission (SRTM) (Farr et al., 2007) and the ASTER Global Digital Elevation Model (ASTER) (Abrams et al., 2002) – and a land use dataset – the Coordination of Information on the Environment Land Cover (CORINE) (Bossard et al., 2000) – were used. A control experiment (CTL) was conducted with the WRF default topography data set – GTOPO30 – and the default land use data set – USGS global 30$''$ vegetation data (USGS30). Some of the more relevant data set attributes are described in Table 1.

Due to the different classification methods used in the CORINE and the USGS global vegetation data, a recategorization was performed to the CORINE data set to be recognisable by the WRF model. The recategorisation process used to convert CORINE into USGS categories is described in Pineda et al. (2004) work.

The performed simulations were grouped into two sets – Control and Lower Boundary Sensitivity tests (LBS) – as can be seen in Table 2.

In order to analyse model results, focusing on the evaluation of the WRF model sensitivity to topography, the difference fields related to precipitation and wind were computed between the experiments and the control simulation. Furthermore, the study domain was divided following the mountain ridge of the island, in order to be able to study the effects of the upslope and downslope flows. Finally, a more detailed study of simulated hourly precipitation and wind was done. Comparison with observed hourly precipitation and wind data, as well as skill analysis for every experiment were performed. To evaluate in detail the impact of using of the new lower boundary conditions datasets, Madeira Island was divided in the following regions, each one including a group of meteorological stations.

NHESSD
1, 5603–5641, 2013

- Mountainous region ⟶ Height greater than 800 m, covering five stations – Areeiro, Bica da Cana, Calheta, Encumeada and Parque Ecológico do Funchal,
- shore region ⟶ Height less than 800 m, with seven stations – Funchal, S. Jorge, Lugar de Baixo, Ponta do Pargo, S. Martinho Machico and Porto Moniz,
- windward region, nine stations – Funchal, Areeiro, Lugar de Baixo, Bica da Cana, Calheta, Encumeada, S. Martinho, Machico and Parque Ecológico do Funchal,
- leeward region, three stations – S. Jorge, Ponta do Pargo and Porto Moniz.

In their study, Luna et al. (2011) have shown that high model resolution enhances the model skill in this particular event. Therefore the present work will focus in the domain with higher resolution – d03.

Even though performance analyses and validation is usually done using state variables such as temperature and pressure, this study is focused on the Madeira extreme precipitation event and, therefore, only this variable together with wind will be analysed.

A total of 12 weather stations were considered, five of which are owned and operated by the Portuguese Meteorological Institute and present only precipitation data – Areeiro, Funchal, Lugar de Baixo, Ponta do Pargo and S. Jorge. The other seven stations are owned and operated by the Madeira Regional Civil Engineer Laboratory and present precipitation and two meter wind speed and direction data – Bica da Cana, Calheta, Encumeada, S. Martinho, Machico, Parque Ecológico do Funchal, Porto Moniz. For both sets of weather stations, data are available on hourly bases, for a period from 20 February 2010, 00:00:00 UTC to 21 February 2010, 00:00:00 UTC. Location and altitude information about these stations are shown in Table 3 and Fig. 3. Furthermore, in order to produce vertical profiles of the atmospheric properties, a meridional cross section was considered at a longitude of 16.93° W, considering all latitudes within the higher resolution domain – d03 – as can be seen in Fig. 3.

In order to analyse the model performance for all simulations and compare them, the following statistical and error measures, relative to observations were calculated (Keyser and Anthes, 1977; Pielke, 2002):

– Deviation of the modelled data in relation to observed values:

$$\Phi'_i = \Phi_i - \Phi_{i,\mathrm{obs}} \tag{1}$$

– Bias, which represents the mean deviation of the modelled data in relation to the observed values:

$$\mathrm{Bias} = \frac{1}{N}\sum_{i=1}^{N}\Phi'_i \tag{2}$$

– The Root Mean Square Error:

$$E = \sqrt{\frac{\sum_{i=1}^{N}\left(\Phi_i - \Phi_{i,\mathrm{obs}}\right)^2}{N}} \tag{3}$$

– The Root Mean Square Error after the removal of a constant bias:

$$E_{\mathrm{UB}} = \sqrt{\frac{\sum_{i=1}^{n}\left[\left(\Phi_i - \overline{\Phi}\right) - \left(\Phi_{i,\mathrm{obs}} - \overline{\Phi_{\mathrm{obs}}}\right)\right]^2}{N}} \tag{4}$$

Discussion Paper | Discussion Paper | Discussion Paper | Discussion Paper |

NHESSD

1, 5603–5641, 2013

WRF sensitivity to lower boundary – extreme precipitation

J. C. Teixeira et al.

Title Page
Abstract Introduction
Conclusions References
Tables Figures
Back Close
Full Screen / Esc
Printer-friendly Version
Interactive Discussion

– Standard deviation for the modelled – Eq. (5) – and observed – Eq. (6) – data:

$$S = \sqrt{\frac{\sum_{i=1}^{n}\left(\phi_i - \overline{\phi}\right)^2}{N}} \quad (5)$$

$$S_{\text{obs}} = \sqrt{\frac{\sum_{i=1}^{n}\left(\phi_{i,\text{obs}} - \overline{\phi_{\text{obs}}}\right)^2}{N}} \quad (6)$$

were i is the temporal index and N is the number of elements of ϕ considered.

The model skill is high when the following criteria are verified:

– $S \approx S_{\text{obs}}$

– $E < S_{\text{obs}}$

– $E_{\text{UB}} < S_{\text{obs}}$

– $\text{Bias}^2 \ll E^2$

3 Results and discussion

3.1 Synoptic pattern evolution

Throughout the period under analysis, the synoptic pattern evolution over Madeira Island shows a rapid transition from high to low pressure systems. Between 19 and 20 February 2010, the surface horizontal pressure gradient was weak and, at the 500 hPa level the island was flanked by a trough on the right and a ridge on its left side and there were two depressions located near the Labrador Sea. By 20 February 2010, these two depressions had deepened and were moving westwards, forming a trough

NHESSD
1, 5603–5641, 2013

at mean sea level with a high on its right side. On 21 February 2010, western flux was imposed by the advection of these low pressure systems to west. Keeping in mind that precipitation analysis is dependent on horizontal model resolution, this discussion is focused only on the third nested domain.

When comparing the synoptic setting of this study with others that evaluate the orographic influence on precipitation (idealized studies by Colle, 2004 and Kunz and Kottmeier, 2006a – and real data study by Kunz and Kottmeier, 2006b), some similarities arise. Madeira Island might be regarded as a singular barrier disturbing the synoptic flow, just as in most idealised experiments. Also, during the simulated period the atmosphere is stable stratified – not shown. Therefore, an enhancement of local precipitation over the windward side of the barrier and less precipitation on their lee side due to the subsidence associated to the gravity waves is expected, as shown by Colle (2004) and Kunz and Kottmeier (2006a). In addition, the mountain crests of Madeira Island located perpendicularly to the main flow forces the air mass to rise as it climbs the windward slope on the southern side of the island, capturing moisture on the orographic induced gravity waves on the northern side. This flow dynamics and its precipitation distribution pattern was also verified and studied by Luna et al. (2011) and Couto et al. (2012).

3.2 Sensitivity to topography

All simulations have the same grid resolution. However, due to the different topography and land use datasets interpolation was performed in order to have consistency with the CTL simulation, thus permitting a direct comparison between simulations.

Figure 4 shows the Madeira Island topography as was used for the CTL simulation (Fig. 4a). Figure 4c and d show the difference between CTL and SRTM (SRTM–CTL) and ASTER (ASTER–CTL), respectively. In addition, the topography of the cross section used in this work for CTL, SRTM and ASTER is shown on the upper right-hand side (Fig. 4b).

NHESSD
1, 5603–5641, 2013

As can be seen, the default topography tends to represent smoother topographic features. On the other hand the high resolution datasets present a better representation of those features with higher peaks and deeper valleys as well as steeper terrain slopes. These characteristics make it a better representation of Madeira Island topography.

With regard to the SRTM and ASTER datasets, both show a similar representation of the island topography, with only slight differences between them at the top of the island and in the mid northern slope.

3.2.1 Wind modelled data

As seen before, topography driven precipitation its highly dependent on flow intensity and direction (Jiang, 2003; Colle, 2004; Kunz and Kottmeier, 2006a). Furthermore, it is known that a change in topography may lead to a change in flow characteristics.

In the beginning of 20 February 2010, the simulated wind flow is perpendicular to Madeira's mountainous ridge – from South – thus originating a deceleration zone upstream Madeira Island, causing flow stagnation near the shore – not shown. Its weak intensity ($\sim 10\,\mathrm{m\,s^{-1}}$) induces weak wind flow splitting and therefore ascent flow is dominant. The strongest winds are reproduced by this model simulation right after the mountainous region – down slope – with an approximate intensity of $20\,\mathrm{m\,s^{-1}}$. Nonetheless, in the central Northern leeward side of the island there is a weak flow zone from variable directions ($< 5\,\mathrm{m\,s^{-1}}$), created by the presence of the mountain ridge – orographic shadow zone. This area suggests the presence of mountain wakes downwind of the higher peaks of the Madeira Island.

Later, at 12:00:00 UTC – not shown – the wind flow becomes more intense ($\sim 20\,\mathrm{m\,s^{-1}}$). This flow intensification enhances the flow splitting, making flow intensity stronger near the Eastern and Western ends of Madeira Island. A proportional intensification of wind intensity after the mountainous region is also noticeable. However, it can be seen that the upwind stagnation zone deepens into the island, becoming closer the island peaks. In addition, on the central Northern leeward side of the island the weak flow zone becomes narrowest due to the flow intensification at the western and eastern island boarders. After 18:00:00 UTC the wind flow weakens and changes direction to West, becoming parallel to the Madeira Island mountainous ridge. At this time flow splitting becomes dominant due to the orientation of the wind in relation to the barrier. Therefore, despite not being shown here, a strong wind flow arise in the Southern and Northern Madeira's shore.

Throughout the day, the difference field for wind direction and intensity maintains its characteristics, with most of them located over Madeira Island and on its leeward side. The difference field between SRTM and ASTER with CTL are very similar, thus only SRTM will be presented.

The difference field for intensity at a ten meter height (shaded) between SRTM and CTL simulations (SRTM–CTL) and direction (SRTM in red arrows and CTL in black arrows) for 20 February 2010 at 12:00:00 UTC are shown in Fig. 5. Here It is possible to see that greater changes are located leeward, after the wind flow passes through the Madeira mountainous crests in an area where, for CTL simulation, the wind intensity was weak, with a negative difference at the left side and a positive difference in the right side. The location of these differences may suggest that there is a displacement of the orographic shadow zone between both SRTM and ASTER simulations when compared to the CTL dataset. There is also an intensification zone – positive difference – for the high resolution topography simulations near Ponta do Pargo. This area is located in the Western end of the Island where the slope is steepest, hence, the use of the higher resolution data changes the model topography over this region of the simulated domain significantly, as can be seen in Fig. 4. This fact may affect the flow splitting causing acceleration in this zone.

Over land it is possible to identify a number of positive and negative differences that remain stationary, thus suggesting a strong relationship to the topographic differences that may change the wind flow path. In fact, and as shown in Fig. 6 where the difference field for mean wind intensity at a ten meter height between SRTM and CTL simulations for 20 February 2010 is shown. In fact, these differences present a strong correlation

NHESSD
1, 5603–5641, 2013

coefficient when compared to their topography difference – 0.606 for SRTM simulation and 0.603 for ASTER.

3.2.2 Precipitation modelled results

As Luna et al. (2011) and Couto et al. (2012) have shown, this particular precipitation event was forced by topography flow lifting – orographic precipitation. Given the effect that a different topography dataset in flow properties, as seen in the previous subsection, differences in precipitation distribution and intensity are also expected.

Figure 7 represents the accumulated precipitation for 20 February 2010 CTL simulation. High amounts of precipitation occur in the centre of Madeira Island near the highest peaks. It is also evident that in the southern part of the island – upstream the main flow – there is a large amount of simulated accumulated precipitation as would be expected. As it encounters the barrier – Madeira Island – the air is forced to rise. The raising moist air cools and creates favourable conditions for precipitation to occur. On the other side of the island – the Northern part – there is a decrease in precipitation due to air subsidence and lower moisture content. Therefore, the simulated accumulated precipitation amounts are reduced in this area. This precipitation distribution and patterns are consistent with those that Luna et al. (2011) and Couto et al. (2012) have described for this particular extreme precipitation event.

When comparing the results of SRTM and ASTER simulations with the CTL it is evident that differences occur over the island. Figure 8 shows the accumulated precipitation difference fields between SRTM and CTL (SRTM–CTL) simulation for 20 February 2010. The pattern of the difference field is similar for both simulations in amplitude and in distribution. Furthermore, it is evident that in the Western part of Madeira Island most of the differences are positive, which shows that there is an increase in simulated precipitation for these simulations. This region of the island is characterised by a a steep slope followed by a plateau with an height of 1400 m that is oriented perpendicular to the main flow. As seen before, SRTM and ASTER simulation have a more detailed topography and, therefore, there is an increase of the terrain slope adjacent to the plateau. Consequently it is plausible that steeper slopes enhances the terrain forcing leading to a stronger air rise that may then lead to an enhancement of topographic driven precipitation.

Centred in Madeira Island, it is possible to observe a negative value of accumulated precipitation difference. This negative isolated difference is associated to a deep valley – Ribeira Brava – located near Lugar de Baixo weather station that extends to the top of Madeira Island. The obtained result in this area is consistent with the expected one. As the new high resolution topography data sets tend to deepen the valleys, the area of terrain forcing the air to rise is reduced which may result in a decrease in precipitation.

The highest peaks of Madeira Island are located in its Eastern region. However, near the eastern shore the slopes are not as steep as in the Western region of the island. When applying the high resolution topography it results in a decrease in precipitation near Madeira shore – negative values of accumulated precipitation difference – and an enhancement of precipitation in the Eastern mountainous regions – positive values of accumulated precipitation difference.

In addition, the correlation between the accumulated precipitation difference and the topography difference for both SRTM and ASTER was determined with values of 0.36 and 0.46, respectively, with a confidence level of 95 %. These values, albeit small (<0.5), show a relation between the change in topography and the precipitation difference distribution.

3.3 Sensitivity to land use

As mentioned before, despite all simulations having the same resolution, the use of different datasets introduces differences in the modelled results. Contrary to topography, land use changes over time scale typical of human activity and, therefore, land use datasets may change significantly every time they are updated. In addition, it must be kept in mind that there is a 13 yr time gap between the USGS and CORINE land use used in this work.

NHESSD
1, 5603–5641, 2013

Figure 9 shows the USGS land use categories field for CTL and CORINE simulations. It is possible to observe that there are differences in Madeira's coastline representation between CTL and CORINE simulations. In fact, CORINE dataset gives a more approximated coastline representation of the Madeira Island geographic features to the numerical model. Furthermore, significant differences in land use categories can be distinguished. For example, contrary to CTL simulation, urban and build-up land category is recognised by the model when CORINE dataset is used. Nonetheless, the area occupied by evergreen broadleaf and dryland cropland is reduced when the CORINE dataset is used. Also, an increase of the area occupied by mixed forest and grassland can be observed. These changes between CTL and CORINE simulation may lead to changes in wind flow proprieties, due to changes in soil roughness length and in precipitation patterns (Chen et al., 2001).

Figure 10 shows the difference field between CORINE and CTL simulations for 10 m wind mean intensity for 20 February 2010. As can be seen, the differences produced by the use of the CORINE land use dataset for this particular precipitation event are small when compared to those produced by the use of a high resolution topography dataset. For mean horizontal wind component intensity, it is possible to observe that in CORINE simulation there is a decrease of wind speed ($\sim 2\,\mathrm{m\,s^{-1}}$) around Madeira Island shore, especially in the Eastern end of the island, where a significant change from shrubland and cropland to urban and mixed forest occurs. On the other hand, an increase of mean wind intensity in the mountainous region of the island can be observed ($\sim 2\,\mathrm{m\,s^{-1}}$). When analysing the area where this wind intensification occurs – Fig. 9 – it is possible to see that a change from an area characterised by the existence of deciduous broadleaf forest in CTL simulation is mostly changed to shrubland and grassland which has a lower roughness length in CORINE, thus reducing surface wind drag over this area (Chen and Dudhia, 2001).

For accumulated precipitation – not shown – the difference values are smaller ($< 20\,\mathrm{mm\,m^{-2}\,day^{-1}}$) than those previously seen for simulations in which topography was changed. Most differences are located upwind Madeira Island with positive

NHESSD
1, 5603–5641, 2013

differences values near Madeira's shore in an area of high density of urban and build-up land in CORINE simulation, and negative differences in the mountainous region.

3.4 Modelled results vs. observed data

The previous analysis of the model results showed that, in this case study, the change to a high resolution lower boundary condition dataset leads to a change in model results for precipitation, wind direction and intensity. However, in order to know which one best represents the atmospheric conditions that were present throughout this event – 20 February 2010 –, the comparison of modelled data with observed data its crucial. Therefore, the analyses of Taylor diagrams and skill charts between the model simulations and observed data was performed.

Figure 11 shows the Taylor diagram for v wind component. This diagram show S, the standard deviation of E (STDE) and R between the modelled simulations results and the observed data of all available stations where wind data were available. It is possible to see that for the v wind component, there is an increase of the correlation for SRTM and ASTER simulations when compared to the CTL simulation – from 0.55 to 0.64 and there is also a lower STDE deviation for these simulations. On the other hand, for the u wind component – not shown – the differences between the simulations are smaller. For this wind component, the use of high resolution topography dataset slightly increases the correlation and standard deviation when comparing to the CTL simulation. However, STDE deviation present little change. For CORINE simulation changes in the statistical properties for both horizontal wind components are negligible, not presenting a significant change when compared to CTL simulation.

In Fig. 12 the Taylor diagram for precipitation is shown. Although the large STDE deviation the model has skill in reproducing the observed precipitation, with most of the skill criteria being met for all the performed simulations – not shown. Furthermore, in the Taylor diagram it is possible to observe that differences between simulations correspond to a small change in standard deviation, with CTL and CORINE simulations having the closest values to the observed standard deviation and SRTM and ASTER simulations showing worse results. Nonetheless, it is possible to observe that SRTM and ASTER simulations present slightly higher STDE deviation. However, there is little change in correlation between the simulations and the observed data when comparing these simulation with the CTL and CORINE. As for wind data the use of an higher resolution and up to date land use information – CORINE simulation – little enhancement of model skill is detected when comparing to the CTL simulation.

A better evaluation of the changes in modelled data caused by the change of the lower boundary can be depicted by analysing the skill charts for the four Madeira sub-regions.

For Mountainous and Shore regions all the simulations present similar skill results. There is poor model skill in reproducing the observed wind variability, specially for the u wind component in all simulations ($S/S_{\rm obs} \sim 3$ for u and $S/S_{\rm obs} \sim 1.5$ for v). Moreover, a better representation of the wind intensity was obtained for u wind component for SRTM and ASTER simulations (lower $E/S_{\rm obs}$ than for the control simulation). However, these simulations present a larger value of $E/S_{\rm obs}$ for the v wind component than the control simulation. On the other hand, for the Shore region in, the use of the high resolution topography and land use datasets enhances mode skill for v variability and intensity. Contrarily, there are no major differences in skill measures between simulations for the u component. For precipitation there is high skill simulating precipitation in the Shore region – every skill criteria is verified – although skill measures for different simulations are identical having only negligible variations. For the Mountainous region there is skill simulating precipitation even though the simulated precipitation variability is larger than the observed one ($S/S_{\rm obs} \sim 1.5$). Furthermore, SRTM and ASTER present the worst skill for this variable in this region.

When separating the domain into windward and leeward regions larger differences between simulations arise. At windward region, there is poor skill in simulating both wind components. As seen for the Mountainous and Shore regions, here the u wind component also presents larger variability than the observations ($S/S_{\rm obs} \sim 1.8$. Nevertheless, SRTM simulation presents a significant enhancement of skill when

NHESSD
1, 5603–5641, 2013

compared with the other simulations, namely there is a decrease of 0.4 S/S_{obs}, E/S_{obs} and E_{UB}/S_{obs}. However there is greater lag between this simulation and the control (larger value for $BIAS^2/E^2$). For v wind component there are only small differences between simulations. At leeward region CTL, CORINE and ASTER simulation present a very poor skill simulating both horizontal wind components – $S/S_{obs} > 4.5$, $E/S_{obs} > 7$, $R < 0$. With the use of the SRTM topography dataset there is a significant improvement of model skill with values for $S/S_{obs} \sim 2$, $E/S_{obs} \sim 2$, $R > 0.3$.

Figure 13 shows the skill chart for precipitation in both windward and leeward regions. In this figure, one can see that for the windward region there is skill in simulating the occurred precipitation despite the slight higher modelled variability when compared to the observed one. Likewise for wind data, only SRTM simulation presents major changes when compared to the control simulation with a significant enhancement of model skill. On the other and, for leeward region the is also skill simulating this atmospheric property despite the lower variability when compared to the observed ($S/S_{obs} < 1$). However, in this region the use of SRTM topography results in poor model skill.

Still, it should be taken into consideration that differences found for skill in these regions are not only caused by the use of a different topography dataset. When applying the criteria for these two regions – windward and leeward – stations located along Madeira ridge are considered to be in the different regions for SRTM, ASTER and CTL. This change may occur due to differences in the location of Madeira's ridge in the SRTM when compared to all other datasets.

4 Concluding remarks

The WRF atmospheric model was used to assess the numerical model sensitivity to the lower boundary conditions in an extreme precipitation event. The event chosen was triggered by the orography and occurred in Madeira Island – Portugal – in 20 February

NHESSD
1, 5603–5641, 2013

2010. The occurred precipitation intensity produced flash floods and mudslides, which had important social and economic consequences.

Three different state of the art high resolution lower boundary condition datasets were use to simulate this event, thereby allowing the evaluation of the sensitivity to lower boundary conditions. The datasets used were the SRTM and ASTER for topography and CORINE for land use. The simulations started at 20 February 2010 and were extended for the following 24 h, thus simulating all the event duration.

Considering the default topography data used by WRF model – GTOPO30 – and the two other new topography datasets introduced in this work – SRTM and ASTER – changes can be observed in topography, albeit all simulations having the same grid resolution. With the use of the high resolution topography datasets there is a deepening of the valleys and higher peaks – changes that can be greater than 100 m – therefore, it may better represent the topographic features of Madeira Island.

Given these differences, a comparison between the performed simulations – CTL, SRTM and ASTER – was made. There, it was possible to see that the use of any of the high resolution topography datasets may lead to changes in wind flow, specially over Madeira Island and in the leeward region. Nonetheless, it was possible to see that these changes are correlated with the differences between the topography datasets. Additionally, changes in precipitation pattern and distribution between CTL, SRTM and ASTER simulations over Madeira Island could also be observed. These changes are related to topographic features, as the change in terrain slope changes terrain forcing, resulting in an intensification of up lifting which may result in an increase of precipitation and vice versa. Thereupon, an increase of precipitation over the Mountainous ridges and a decrease of precipitation accumulated amounts over the valley, are consistent with changes associated with the topographic forcing.

Comparing the simulated wind and precipitation results against observations it was possible to see that there is low model skill for u and v wind components over Madeira Island for all the performed simulations. Furthermore, when using high resolution topography datasets a slight enhancement of model skill can be observed.

NHESSD
1, 5603–5641, 2013

However, this enhancement is small. Considering the precipitation data, it could be seen that there is a high model skill. However, the observed variability for precipitation is overestimated by the model for all simulations. For this variable, SRTM and ASTER simulations presented a decrease in model skill when compared to the control simulation. However this decrease is small.

To evaluate these changes with more detail a study considering four distinct Madeira Island regions was performed, namely Mountainous, Shore, windward and leeward regions. These results show that, concerning the simulation of wind flow, the model performs best for altitudes higher than 800 m for all the simulations. It could also be seen that, a small enhancement of model skill can be achieved for the leeward region when using the SRTM topography dataset. For precipitation data the opposite result can be observed and there is high model skill to simulate precipitation for altitudes lower than 800 m for all performed simulations. Furthermore, a significant improvement of model skill on the leeward region was achieved using the SRTM topography dataset. On the other side, for windward region, albeit the small differences between simulations, SRTM present a lower model skill. Nonetheless, one should take into consideration that the differences found for skill in these regions – specially windward and leeward – are not only caused by the use of a different topography dataset, but also due to the fact that stations located along Madeira ridge are considered to be in the different regions for SRTM, ASTER and CTL as result of the differences in the location of Madeira's ridge in the SRTM when compared to all other datasets.

Sensitivity tests were also performed with a high resolution land use dataset – CORINE. However, this dataset gives little changes to model results when compared to the control simulation.

Given this, one may conclude that the use of an high resolution dataset within WRF model leads to changes to model results for this particular orographic extreme precipitation event. Furthermore, when comparing to observed data it can be concluded that, overall, there is little gain of model skill when using any of the high resolution lower boundary conditions datasets. However, when analysing specific regions of Madeira Island, one can see that SRTM and ASTER gives an improvement of model skill on the windward region for precipitation and on leeward region for wind. On the other hand, decrease of model skill simulating precipitation can be observed. Therefore the used of high resolution datasets in numerical weather model may improve model skill in simulating topography force processes.

Acknowledgements. This study was supported by FEDER funds through the Programa Operacional Factores de Competitividade – COMPETE and by Portuguese national funds through FCT – Fundação para a Ciencia e a Tecnologia, within the framework of Project Urban Atmospheric Quality, Climate Change and Resilience. EXCL/AAG-MAA/0383/2012.

References

Abrams, M., Hook, S., and Ramachandran, B.: ASTER User Handbook* Version 2, Jet Propulsion Laboratory, 4800, 135 pp., 2002. 5608

Bossard, M., Feranec, J., and Otahel, J.: CORINE land cover technical guide – Addendum 2000, European Environment Agency, 2000. 5608

Chen, F. and Dudhia, J.: Coupling an advanced landsurface/hydrology model with the Penn State/NCAR MM5 modeling system. Part I: Model description and implementation, Mon. Weather. Rev., 129, 569–585, 2001. 5608, 5617

Chen, F., Warner, T., and Manning, K.: Sensitivity of orographic moist convection to landscape variability: a study of the Buffalo Creek, Colorado, flash flood case of 1996, J. Atmos. Sci., 58, 3204–3223, 2001. 5606, 5617

Chou, M. D. and Suarez, M.: A thermal infrared radiation parameterization for atmospheric studies, NASA/TM, 2001-104606, 55, 2001. 5607

Colle, B.: Sensitivity of orographic precipitation to changing ambient conditions and terrain geometries: an idealized modeling perspective, J. Atmos. Sci., 61, 588–606, 2004. 5604, 5605, 5612, 5613

Couto, F. T., Salgado, R., and Costa, M. J.: Analysis of intense rainfall events on Madeira Island during the 2009/2010 winter, Nat. Hazards Earth Syst. Sci., 12, 2225–2240, doi:10.5194/nhess-12-2225-2012, 2012. 5606, 5612, 5615

Farr, T. G., Rosen, P. A., Caro, E., Crippen, R., Duren, R., Hensley, S., Kobrick, M., Paller, M., Rodriguez, E., Roth, L., Seal, D., Shaffer, S., Shimada, J., Umland, J., Werner, M., Oskin, M., Burbank, D., and Alsdorf, D.: The shuttle radar topography mission, Rev. Geophys., 45, 1–33, 2007. 5608

Fragoso, M., Trigo, R. M., Pinto, J. G., Lopes, S., Lopes, A., Ulbrich, S., and Magro, C.: The 20 February 2010 Madeira flash-floods: synoptic analysis and extreme rainfall assessment, Nat. Hazards Earth Syst. Sci., 12, 715–730, doi:10.5194/nhess-12-715-2012, 2012. 5606

Ghafarian, P., Azadi, M., Meshkatee, A. H., and Farahani, M. M.: Numerical simulation of the impact of Anatolian and Caucasus Mountains on the precipitation distribution over the Black Sea, Nat. Hazards Earth Syst. Sci., 12, 607–613, doi:10.5194/nhess-12-607-2012, 2012. 5605

Grumm, R.: The Madeira Island Floods of 20 February 2010, National Weather Service of the United States of America, available at: http://cms.met.psu.edu/sref/severe/2010/20Feb2010.pdf, 2010. 5606

Hong, S. Y. and Lim, J. O. J.: The WRF single-moment 6-class microphysics scheme (WSM6), J. Korean Meteor. Soc., 42, 129–151, 2006. 5607

Janjić, Z. I.: The step-mountain coordinate: physical package, Mon. Weather. Rev., 118, 1429–1443, 1990. 5608

Janjić, Z.: Nonsingular implementation of the Mellor–Yamada level 2.5 scheme in the NCEP Meso model, NCEP Office Note, 437, 61, 2002. 5607

Jiang, Q.: Moist dynamics and orographic precipitation, Tellus A, 55, 301–316, 2003. 5604, 5605, 5613

Keyser, D. and Anthes, R. A.: The applicability of a mixed-layer model of the planetary boundary layer to real-data forecasting, Mon. Weather. Rev., 105, 1351–1371, 1977. 5610

Kunz, M. and Kottmeier, C.: Orographic enhancement of precipitation over low mountain ranges. Part I: Model formulation and idealized simulations, J. Appl. Meteorol. Clim., 45, 1025–1040, 2006a. 5604, 5605, 5612, 5613

Kunz, M. and Kottmeier, C.: Orographic enhancement of precipitation over low mountain ranges. Part II: Simulations of heavy precipitation events over southwest Germany, J. Appl. Meteorol. Clim., 45, 1041–1055, 2006b. 5605, 5612

Luna, T., Rocha, A., Carvalho, A. C., Ferreira, J. A., and Sousa, J.: Modelling the extreme precipitation event over Madeira Island on 20 February 2010, Nat. Hazards Earth Syst. Sci.,

NHESSD
1, 5603–5641, 2013
WRF sensitivity to lower boundary – extreme precipitation
J. C. Teixeira et al.

11, 2437–2452, doi:10.5194/nhess-11-2437-2011, 2011. 5606, 5607, 5608, 5609, 5612, 5615
Maussion, F., Scherer, D., Finkelnburg, R., Richters, J., Yang, W., and Yao, T.: WRF simulation of a precipitation event over the Tibetan Plateau, China – an assessment using remote sensing and ground observations, Hydrol. Earth Syst. Sci., 15, 1795–1817, doi:10.5194/hess-15-1795-2011, 2011. 5605
Mlawer, E. J., Taubman, S. J., Brown, P. D. anf Lacono, M. J., and Clough, S. A.: Radiative transfer for inhomogeneous atmosphere: RRTM, a validated correlated-k model for the long-wave, J. Geophys. Res., 102, 16663–16682, 1997. 5607
NCEP: The GFS Atmospheric Model, NCEP Office Note 442, Global Climate and Weather Modeling Branch, 2003. 5607
Pielke, R.: Mesoscale Meteorological Modeling, 78, 676 pp., 2002. 5610
Pineda, N., Jorba, O., Jorge, J., and Baldasano, J.: Using NOAA AVHRR and SPOT VGT data to estimate surface parameters: application to a mesoscale meteorological model, Int. J. Remote. Sens., 25, 129–143, 2004. 5608
Shi, X., Wang, Y., and Xu, X.: Effect of mesoscale topography over the Tibetan Plateau on summer precipitation in China: a regional model study, Geophys. Res. Lett., 35, L19707, doi:10.1029/2008GL034740, 2008. 5605
Skamarock, W. C., Klemp, J. B., Dudhia, J., Gill, D. O., Barke, D. M., Wang, W., and Powers, J. G.: A Description of the Advance Reaserch WRF version 3, NCAR Technical Note, 2008. 5607
Vrochidou, A.-E. K. and Tsanis, I. K.: Assessing precipitation distribution impacts on droughts on the island of Crete, Nat. Hazards Earth Syst. Sci., 12, 1159–1171, doi:10.5194/nhess-12-1159-2012, 2012. 5605

NHESSD
1, 5603–5641, 2013

WRF sensitivity to lower boundary – extreme precipitation

J. C. Teixeira et al.

Table 1. Topography (bold) and land use data set attributes.

	Resolution	Year	Soil Categories
GTOPO30	**30″**	**1996**	**NA**
SRTM	**3″**	**2005**	**NA**
ASTER	**1″**	**2009**	**NA**
USGS30	30″	1993	25
CORINE	100 m	2006	44

NHESSD

1, 5603–5641, 2013

WRF sensitivity to lower boundary – extreme precipitation

J. C. Teixeira et al.

Table 2. Lower boundary conditions and microphysics schemes used on WRF simulation.

Simulation Set	Run	Lower Boundary Condition
Control	CTL	GTOPO30 + USGS30
LBS	SRTM	SRTM + USGS30
	ASTER	ASTER + USGS30
	CORINE	GTOPO30 + CORINE

NHESSD
1, 5603–5641, 2013

Table 3. Weather Station information used to evaluate model skill – Operated by the Regional Civil Engineer Laboratory (bold) and Portuguese Meteorological Institute.

Location	Latitude (°)	Longitude (°)	Altitude (m)
Lugar de Baixo	32.67	−17.08	15
Funchal	32.64	−16.89	58
Machico	**32.73**	**−16.78**	**170**
S. Jorge	32.83	−17.90	185
S. Martinho	**32.65**	**−16.94**	**250**
Ponta do Pargo	32.81	−17.26	312
Porto Muniz	**32.84**	**−17.19**	**675**
Encumeada	**32.75**	**−17.02**	**1017**
Calheta	**32.77**	**−17.18**	**1020**
P.E. Funchal	**32.70**	**−16.90**	**1300**
Bica da Cana	**32.76**	**−17.06**	**1600**
Areeiro	32.71	−16.91	1610

NHESSD
1, 5603–5641, 2013

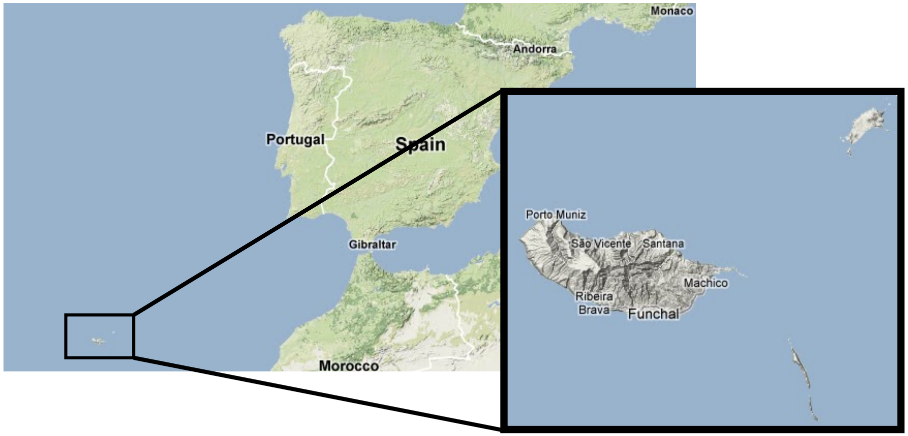

Fig. 1. Study area map showing the Madeira archipelago location in the Atlantic Ocean, maps from googlemaps.com.

NHESSD
1, 5603–5641, 2013

WRF sensitivity to lower boundary – extreme precipitation

J. C. Teixeira et al.

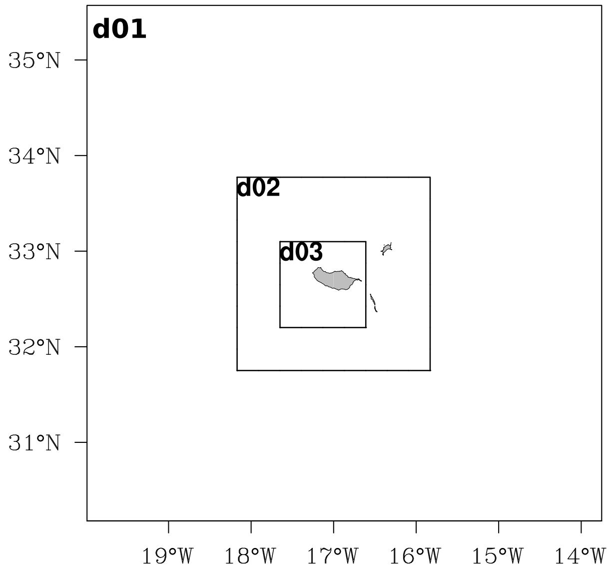

Fig. 2. Three nested model domains used in WRF.

NHESSD
1, 5603–5641, 2013

WRF sensitivity to lower boundary – extreme precipitation

J. C. Teixeira et al.

Fig. 3. Location of the weather stations in Madeira Island (blue doted – Portuguese Meteorological Institute; White doted – Madeira Regional Civil Engineer Laboratory) and the cross section at 16.93° W used in this work (red line).

NHESSD
1, 5603–5641, 2013

NHESSD
1, 5603–5641, 2013

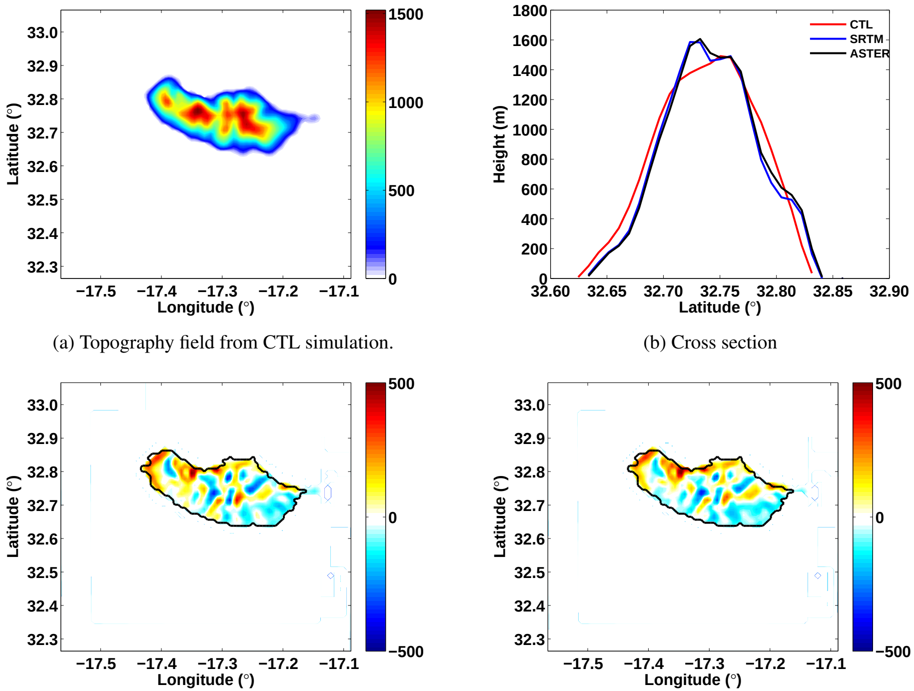

(a) Topography field from CTL simulation.
(b) Cross section
(c) SRTM - CTL
(d) ASTER - CTL

Fig. 4. Topography field for CTL simulation (m) **(a)** and topography cross section for the three data sets, CTL (red), SRTM (blue) and ASTER (black) simulations **(b)**, and difference fields (m) between both high resolution topography datasets and the control topography for domain d03 at a resolution of one kilometre **(c)** and **(d)**.

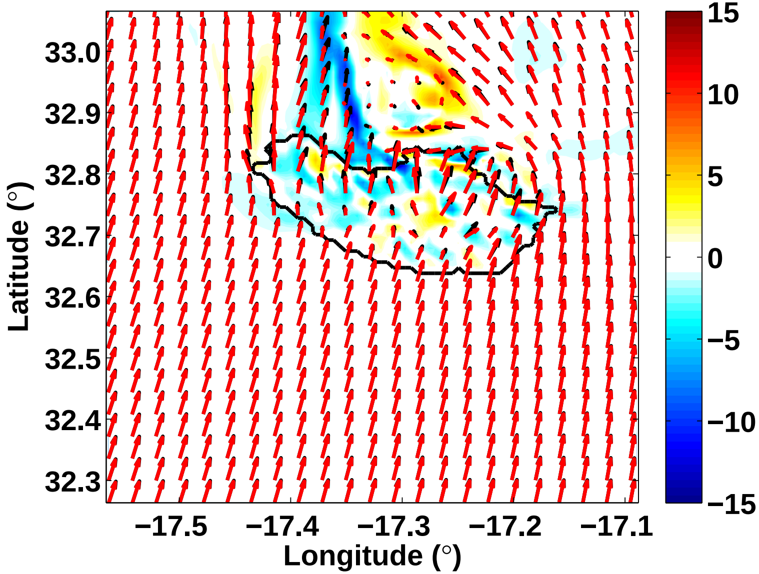

Fig. 5. Difference field for intensity (m s^{-1}) at a ten meter hight (shaded) between SRTM and CTL simulations and wind direction for SRTM (red arrows) and CTL simulations (black arrows) for 20 February 2010, at 12:00:00 UTC.

NHESSD
1, 5603–5641, 2013

WRF sensitivity to lower boundary – extreme precipitation

J. C. Teixeira et al.

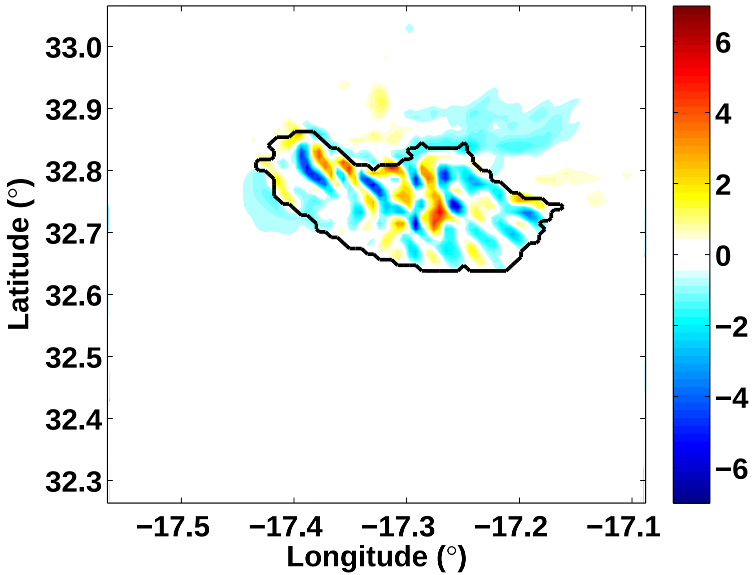

Fig. 6. Difference field for mean wind intensity ($m\,s^{-1}$) at a ten meter height between SRTM and CTL simulations for 20 February 2010.

NHESSD
1, 5603–5641, 2013

WRF sensitivity to lower boundary – extreme precipitation

J. C. Teixeira et al.

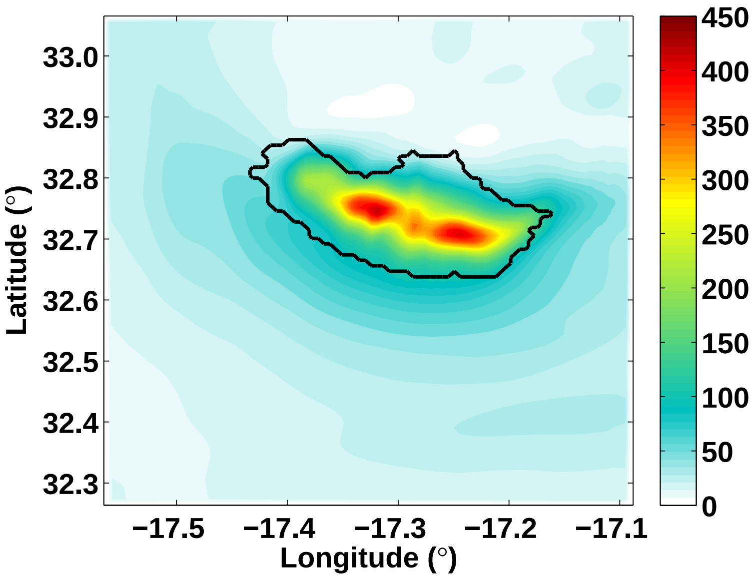

Fig. 7. Accumulated precipitation (mm day^{-1}) for 20 February 2010 for control simulation.

NHESSD
1, 5603–5641, 2013

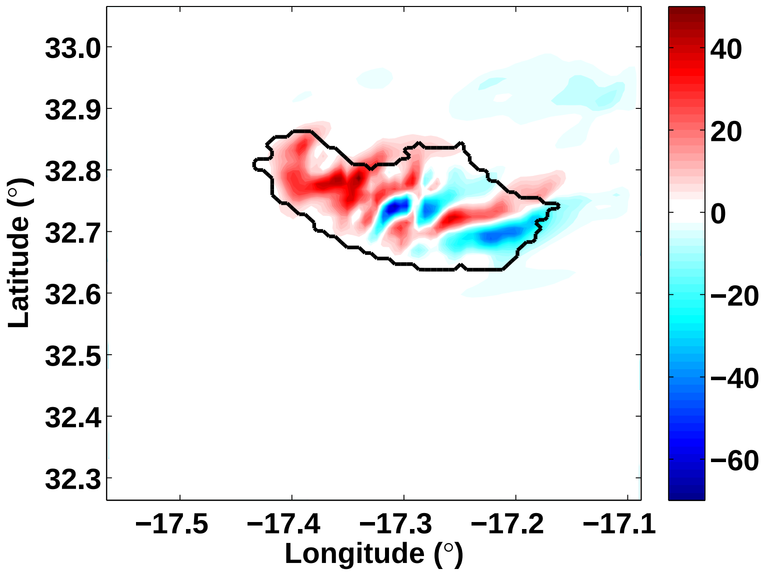

Fig. 8. Difference fields for accumulated precipitation (mm day^{-1}) between SRTM and CTL simulation for 20 February 2010.

NHESSD

1, 5603–5641, 2013

WRF sensitivity to lower boundary – extreme precipitation

J. C. Teixeira et al.

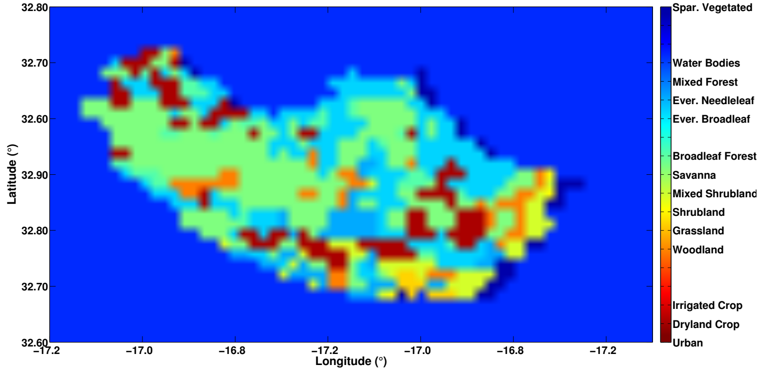

(a) CTL simulation.

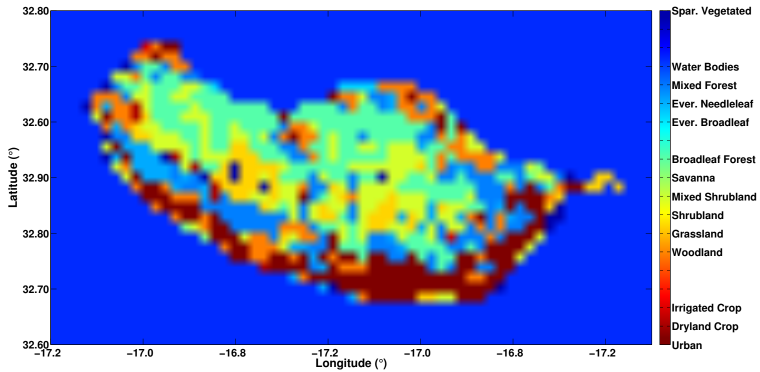

(b) CORINE simulation

Fig. 9. USGS land use categories field based on the USGS **(a)** and in CORINE land use dataset **(b)**.

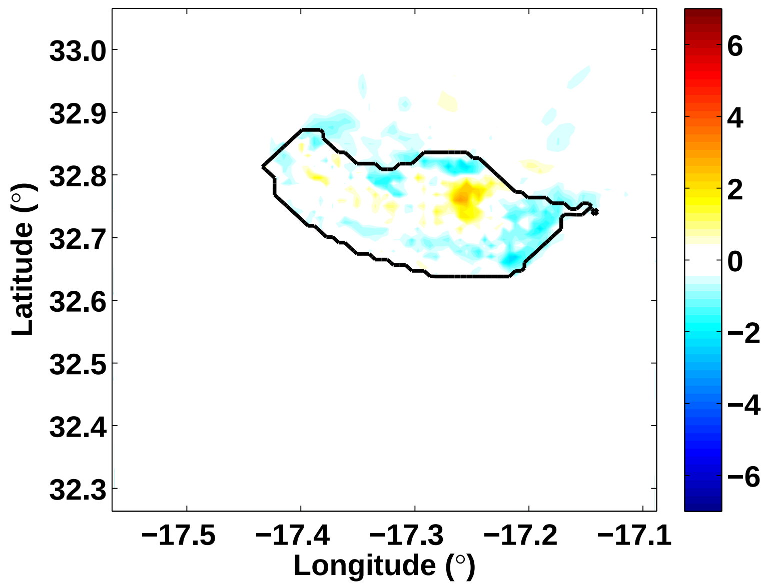

Fig. 10. Difference fields between CORINE and CTL simulations for 10 m wind mean intensity – horizontal components – 20 February 2010.

NHESSD
1, 5603–5641, 2013

WRF sensitivity to lower boundary – extreme precipitation

J. C. Teixeira et al.

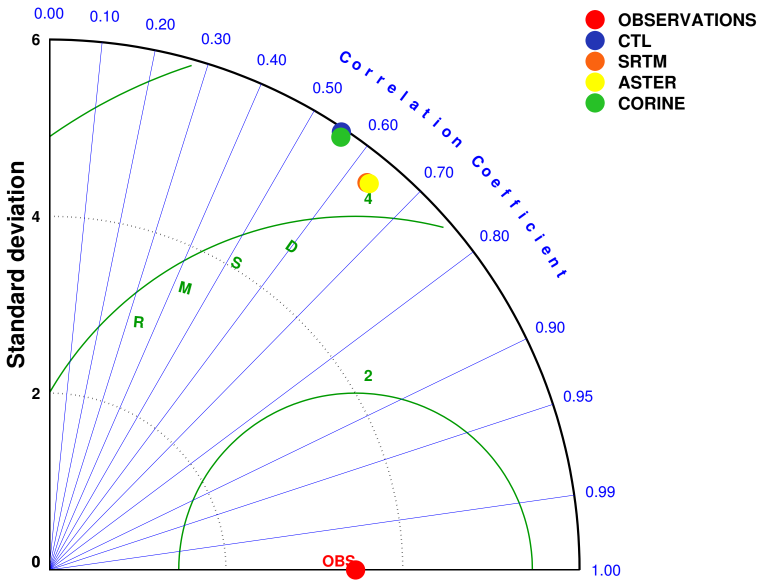

Fig. 11. Taylor diagrams for *v* wind components – green curved lines represent the STDE.

NHESSD
1, 5603–5641, 2013

WRF sensitivity to lower boundary – extreme precipitation

J. C. Teixeira et al.

Title Page
Abstract | Introduction
Conclusions | References
Tables | Figures
◀I | ▶I
◀ | ▶
Back | Close
Full Screen / Esc
Printer-friendly Version
Interactive Discussion

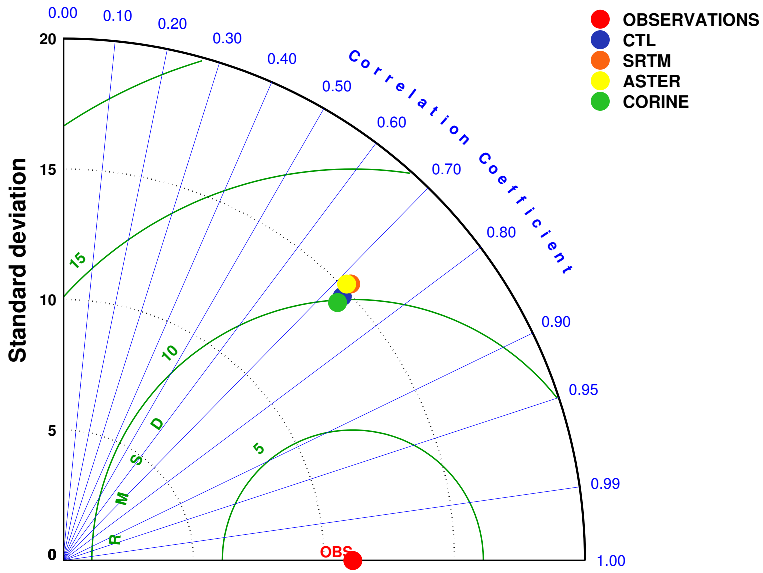

Fig. 12. Taylor diagram for precipitation – green curved lines represent the STDE.

NHESSD
1, 5603–5641, 2013

WRF sensitivity to lower boundary – extreme precipitation

J. C. Teixeira et al.

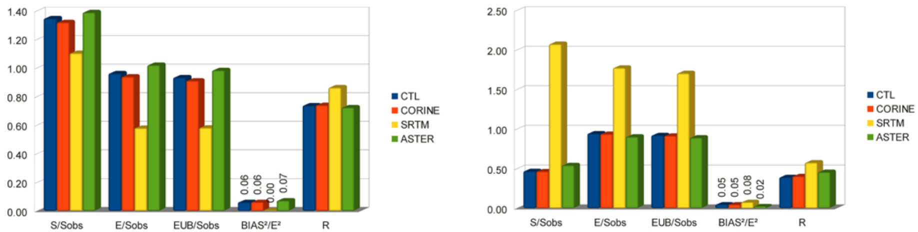

(a) Windward region

(b) Leeward region

Fig. 13. Precipitation skill chart for the stations located windward **(a)** and leeward **(b)** regions.

NHESSD

1, 5603–5641, 2013